NAS - CR 72039

Eighth Quarterly Report

for

1 April 1966 to 1 July 1966

DETERMINATION OF ELEVATED-TEMPERATURE FATIGUE DATA ON REFRACTORY ALLOYS IN ULTRA HIGH VACUUM

Prepared by:

C. R. Honeycutt, T. F. Martin, and J. C. Sawyer

Prepared for:

NATIONAL AERONAUTICS AND SPACE ADMINISTRATION
CONTRACT NO. NAS 3-6010

TECHNICAL MANAGEMENT

Paul E. Moorhead
Space Power Systems Division
NASA- Lewis Research Center

July 15, 1966

TRW EQUIPMENT LABORATORIES
TRW INC.
23555 Euclid Avenue
Cleveland, Ohio 44117

FOREWORD

The work described herein is being performed by TRW Inc. under the sponsorship of the National Aeronautics and Space Administration under Contract NAS 3-6010. The purpose of this study is to obtain fatigue life data on refractory metal alloys for use in designing space power systems.

The program is administered for TRW Inc by E. A. Steigerwald, program manager. C. R. Honeycutt, T. F. Martin, and J. C. Sawyer are the principal investigators and the NASA technical program manager is P. E. Moorhead

Prepared by C. R. Honeycutt
C. R. Honeycutt
Research Metallurgist

Prepared by T. F. Martin
T. F. Martin
Research Physicist

Prepared by J. C. Sawyer
J. C. Sawyer
Sr. Research Metallurgist

Approved by E. A. Steigerwald
E. A. Steigerwald
Research Supervisor

Approved by G. V. Guarnieri
G. V. Guarnieri, Manager
Materials Research & Development

ABSTRACT

During this report period, specimens of TZM alloy having various notch configurations were fatigue tested at 2000°F (1093°C) to determine the effect of notch geometry on fatigue strength. Above a notch factor of approximately two, stress values for fatigue failures calculated from classical notch theory produced values which were apparently below those obtained on smooth specimens.

Tension-tension fatigue tests conducted on TZC alloy smooth specimens at 2000°F (1093°C) with a 20 Ksi ($1.38 \times 10^8 N/m^2$) static load and A ratios of 0.1 to 0.4 indicated that the presence of the dynamic load significantly increased the total creep extension. At 2000°F (1093°C) as much as 2.8% creep has been observed in 59 hours at a peak stress of 27.2 Ksi ($1.88 \times 10^8 N/m^2$).

TABLE OF CONTENTS

I INTRODUCTION

The purpose of this investigation is to generate fatigue data for refractory alloys at elevated temperatures in ultra-high vacuum environments. The ultimate objective is to determine whether fatigue life or creep is the limiting design parameter in turbine applications involving space electric power systems.

Previous reports have described the design and construction of equipment for conducting fatigue tests in vacuum chambers at temperatures up to 3000°F (1649°C). The application of the cyclic stress is accomplished by a piezoelectric transducer operating at approximately 20 kHz in an ultra high vacuum system. Using this apparatus fatigue tests have been conducted on notched specimens (K_T = 1.75) of TZM at 1800°F (982°C) and TZC at 2000°F (1093°C). Smooth fatigue tests have also been performed on both TZC and TZM alloys under tension-compression and tension-tension conditions. The results indicate that the fatigue strength, predicted from the notch tests on the specimens with a stress concentration factor of 1.75, is significantly less than that experimentally obtained with smooth specimens.

During this report period additional tests were conducted in an effort to determine the reason for the difference between smooth and notch test results. The influence of a superimposed dynamic stress on the creep experienced in a smooth specimen was also evaluated.

II MATERIALS AND PROCEDURE

The specific form, heat numbers, and compositions of the TZM and TZC molybdenum-based alloys utilized in the tests conducted during this quarter are summarized in Table 1. All fatigue specimens prepared from these alloys were recrystallized by vacuum annealing for 1 hour at 2850°F (1566°C) for TZM, or at 3092°F (1700°C) for TZC. The TZM alloy has been used to investigate the effect of notch geometry on fatigue strength. Fatigue specimens of TZC bar (No. 4230-2) and plate (Heats M-89 and M-91) have been tested for fatigue strength and creep properties under combined dynamic-static loading conditions.

TABLE 1

CHEMICAL COMPOSITION OF ALLOYS TESTED

Material	Form	Vendor	Heat	Composition - weight % Mo	Zr	Ti	C	Condition
TZM	1/2" Diameter Bar	Climax	7468	Bal.	0.09	0.50	0.022	Stress relieve, 1/2 hour at 1232°C; anneal, 1 hour at 1566°C
TZC	1/2" Diameter Bar	Climax	4230-2	Bal.	0.29	1.35	0.089	Stress relieve, 1/2 hour at 1315°C; anneal, 1 hour at 1700°C
TZC	0.60" Cross-rolled Plate	G.E.	M-89	Bal.	0.20	1.45	0.13	Anneal at TRW 1700°C 1 hour, ASTM grain size 1 to 4
TZC	0.60" Cross-rolled Plate	G.E.	M-91	Bal.	0.18	1.25	0.14	Anneal at TRW 1700°C 1 Hour, ASTM grain size 4 to 6

The procedure for conducting the fatigue tests has been described in detail in the Seventh Quarterly Report (NAS CR-54983). The test method utilizes a resonant system operating at 20 kHz in a vacuum of 1×10^{-8} Torr or better prior to heat-up and which never exceeds 1×10^{-6} Torr during the heat-up operation.

A W-3%Re/W-25%Re thermocouple placed approximately 1/8 inch from the surface at the specimen midpoint is used for temperature measurement. Due to breakage produced by the vibration, the thermocouple cannot be attached directly to the specimen. The temperature is stabilized for approximately two hours prior to the application of the cyclic load.

As a result of the application of the high frequency cyclic load, heating of the fatigue specimen takes place. For a given material, the degree of heating is dependent upon the power applied to the system. At high stress levels where significant heating of the specimen occurred, test times were on occasion so short that a readjustment of the furnace temperature to compensate for self heating could not be accomplished. At low values of applied dynamic stress, the temperature increase was very slight and no adjustment of furnace temperature was usually necessary. To be consistent, the procedure up to this time has been to set the furnace temperature at some constant value (usually 2000°F (1093°C) for the duration of the test and to measure the temperature increase of the test specimen with an L-N optical pyrometer.

It is recognized that this procedure embodies an inherent and undesirable temperature variability. For this reason test procedures will be developed wherein the furnace temperature is adjusted to compensate for the temperature increase so as to permit tests to be conducted at a constant specimen temperature.

The applied dynamic stress produced by the ultrasonic vibration was determined from displacement measurements made directly on the specimen with a cathetometer. In smooth specimens the maximum dynamic stress was calculated from the equation:

$$\sigma_{max} = \frac{2\pi}{\lambda} \delta_x \quad E \quad \text{Cosec} \frac{2\pi x}{\lambda} \qquad (1)$$

where σ_{max} is the peak dynamic stress, λ is the resonant wave length, δ_x is the vibration amplitude measured at a distance x from the node in the specimen gauge length, and E is the dynamic elastic modulus.

In notch specimens the peak dynamic stress was determined from the equation:

$$\sigma_{max} = \left[K_T \left(\frac{D}{d}\right)^2\right] \left(\frac{2\pi}{\lambda} \delta_x E \operatorname{Cosec} \frac{2\pi\chi}{\lambda}\right) \qquad (2)$$

where the last group has the same meaning as in equation (1), K_T is the theoretical static stress concentration factor, and (D/d) is the ratio of the major-to-minor diameters in the notch specimen. The parameter $K_T (D/d)^2$ has been defined as the notch factor and it has been used to represent the total increase in stress produced by the notch.

III RESULTS AND DISCUSSION

A. Effect of Notch Geometry

A comparison of notch and smooth fatigue data obtained for molybdenum alloys tested at A approaching 00* indicated that the smooth fatigue strength is significantly higher than the fatigue strength obtained in a notch specimen with a notch factor ($K_T D^2/d^2$) of 3.93. In an effort to identify the cause for this difference in fatigue strength from that calculated for the notched specimens, fatigue tests of TZM (Heat 7468) were conducted on both smooth and notched specimens of various geometries at 2000°F (1093°C) and an A ratio of 00. The specimen configuration is shown in Figure 1 while the detailed geometry variations are presented in Figure 2. In addition, a smooth specimen (notch factor equal to unity) was also included in the evaluations.

The data obtained from the tests on the specimens of varying notch geometry are summarized in Table 2 and plotted in Figure 3. If the notch factor accurately defines the influence of the notch on fatigue life, then the peak stress calculated from equation (2) should be a constant independent of notch geometry. The results, however, indicate that above a notch factor ($K_T D^2/d^2$) of approximately two, a systematic variation exists between the peak fatigue stress and the notch factor, with higher factors producing a greater degradation in strength.

---

* The A ratio is the dynamic stress amplitude divided by the mean stress amplitude.

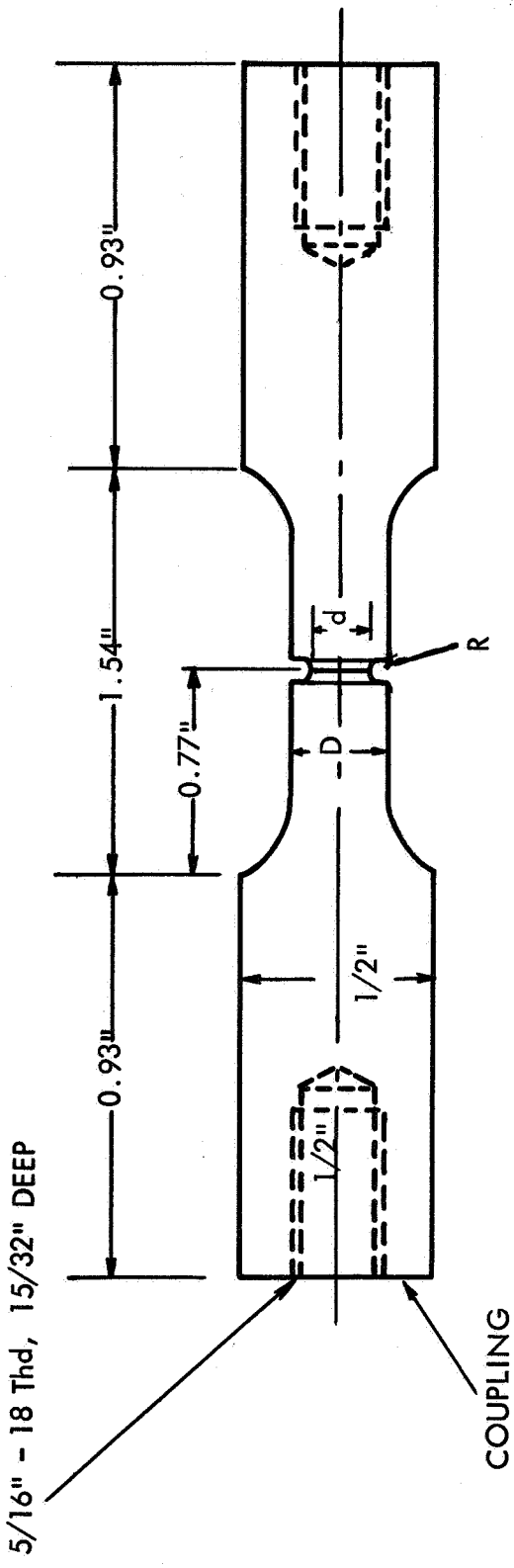

FIGURE 1 GEOMETRY OF NOTCH FATIGUE SPECIMEN

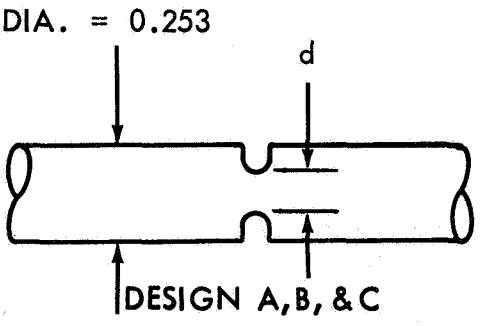

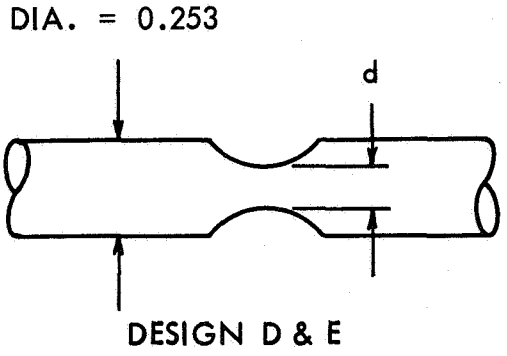

	MINOR DIAMETER (IN.) d	NOTCH RADIUS (IN.) R	STRESS CONC. FACTOR (K_T)	NOTCH FACTOR $K_T (D/d)^2$
A	0.174	0.032	1.75	3.93
B	0.228	0.032	1.91	2.25
C	0.196	0.031	1.81	3.17
D	0.174	0.253	1.10	2.41
E	0.228	0.253	1.16	1.44

FIGURE 2 DESIGN OF SPECIMEN CONFIGURATIONS USED FOR NOTCH EVALUATION STUDIES

TABLE 2

Summary of Notched Fatigue Tests with Various Notch Configurations Using Specimens of TZM (Heat 7468) Recrystallized One Hour at 2850°F (1566°C), Ambient Temperature 2000°F (1093°C), Vacuum Environment (<1 x 10^{-7} Torr)

Specimen	Notch* Design	$\left(\frac{D}{d}\right)^2 K_T$	Peak Total Stress Ksi	Static *** Stress Ksi	Failure Time-Hrs.	Cycles to Failure	Specimen**** Temperature Increase, °F
50	A	3.93	8.24	1.33	~0.15	1.0×10^7	-
51	A	3.93	7.81	1.33	7.60	5.3×10^8	11
53	Smooth	1.00	8.54	0.34	>357.00	$>2.5 \times 10^{10}$	111
53	Smooth	1.00	8.43	0.34	> 32.60	$>2.3 \times 10^9$	157
54	B	2.25	12.70	0.76	>16.90	$>1.2 \times 10^9$	26
54	B	2.25	16.70	0.76	1.60	1.1×10^8	36
55	B	2.25	14.71	0.76	1.37	9.6×10^7	58
56	C	3.17	11.95	1.07	1.25	8.6×10^7	17
57	C	3.17	11.85	1.07	16.60	1.2×10^9	0
58	D	2.41	21.27**	0.82	24.80	1.7×10^9	48
59	D	2.41	13.65	0.82	19.80	1.4×10^9	69
60	E	1.44	11.85	0.49	102.60	7.0×10^9	78
61	E	1.44	17.54	0.49	23.40	1.6×10^9	100
53N	E	1.44	} To be tested				
62	Smooth	1.00					
63	Smooth	1.00					

* See Figure 2 for notch design.

** Asymmetric vibration - data not plotted.

*** Stress resulting from lower half of vibration train and transducer assembly.

**** True test temperature is specimen temperature increase plus 2000°F.

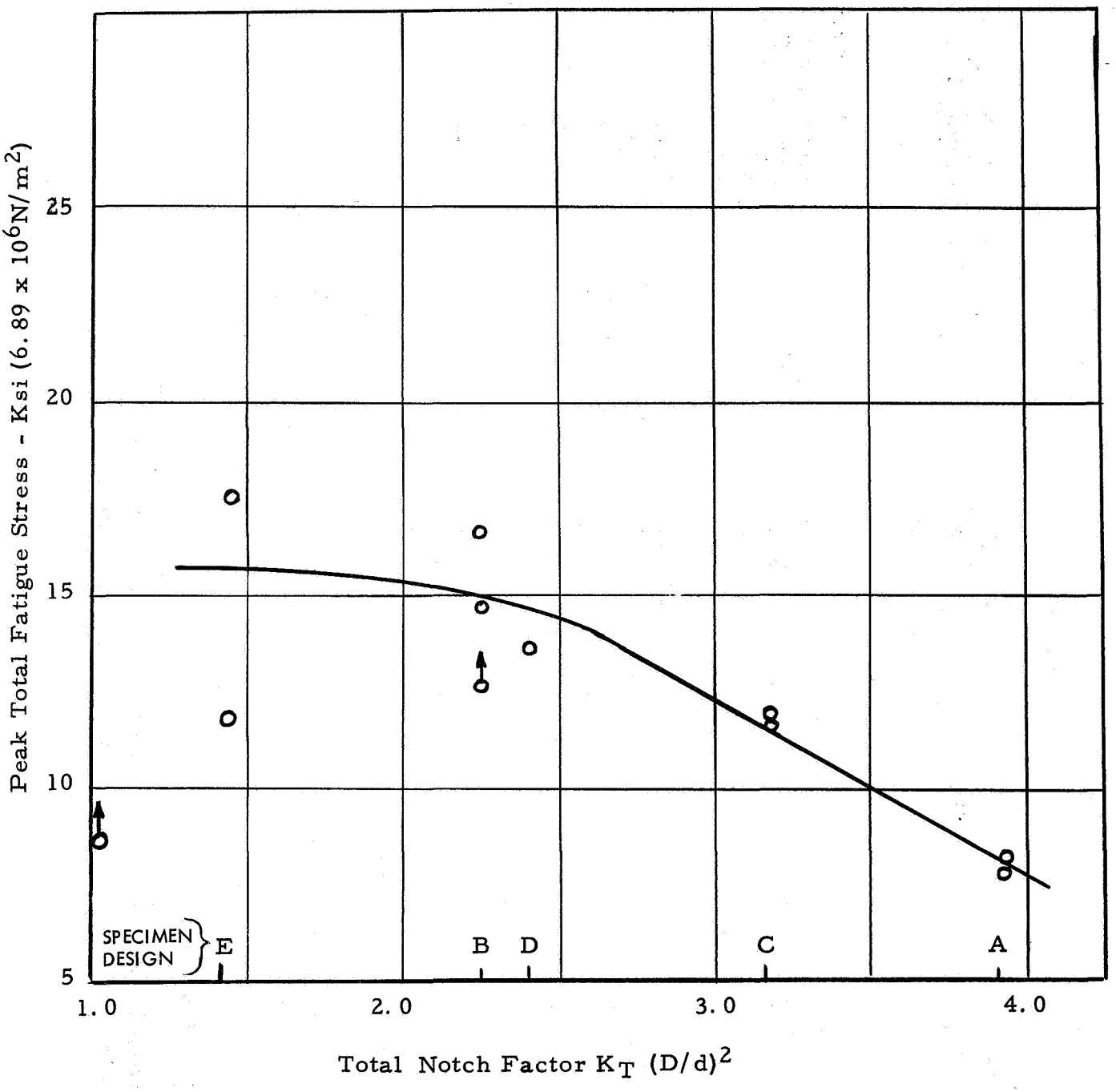

FIGURE 3 VARIATION OF FATIGUE STRESSES WITH NOTCH FACTOR FOR FAILURE AT~10^9 CYCLES. AMBIENT TEMPERATURE 2000°F, VACUUM ENVIRONMENT <1 X 10^{-7} TORR.

Metallographic examination of the notch-fatigue specimens indicated that a well-defined substructure existed along the fracture path. This effect is illustrated in Figures 4 and 5 for specimens tested at 2000°F (1093°C) and an A ratio of ∞. During testing the fatigue crack propagates approximately half-way through the specimen cross-section. The specimens are then broken manually to allow examination of the fracture surface. As shown in Figure 5 the presence of the substructure is uniquely associated with the fatigue crack. The rapid fracture produced on the specimen after removal from the apparatus gave no indication of the substructure indicating that the microstructural effect is not an artifact and can be directly attributed to the fatigue conditions.

Examination was conducted on sections through the fatigue cracks in TZM specimens having notch factors of 3.93, 2.41, 2.25, and 1.44 (specimens 51, 59, 55, and 61). The purpose was to determine whether the substructure varied in relation to the notch factor. These results shown in Figure 6 indicate that a noticeable amount of substructure was present only near the fatigue surface for the specimens with $K_T > 2.0$. In the case of specimens TZM Nos. 59, and 61 (Figures 6B and 6D) which had relatively large notch radii, a precipitate appears to be preferentially located throughout the matrix in the region of the notch. From these observations, the generation of substantial amounts of substructure along the fatigue crack does not occur at notch factors below 2.0, which corresponds to the position where the fatigue life is essentially independent of the notch factor.

Although the mechanism for the formation of the substructure still requires identification, post test microhardness measurements indicate that the substructure is harder than the base material and suggest that a localized strain induced precipitation has occurred at the crack tip to decrease the fatigue strength in the sharply-notched specimens. In the specimens with a relatively mild notch ($K_T\ D^2/d^2 < 2$) a precipitate appears to be more widely distributed about the notch area and the region of hardness increase is also more extensive. Microhardness measurements taken from the notch region and the base material indicate that a hardness increase from 297 to 397 Knoop has occurred in the vicinity of the fatigue fracture (see Figure 7). Along with the localization of strain a localized temperature increase should also occur at the notch tip and this could be contributing to the observed effect. Additional electron-microscopy studies are being conducted in an attempt to further define the mechanism for the formation of the substructure.

The results obtained with various notch geometries indicate that the notch fatigue tests at an A ratio of ∞ should be conducted with specimens having notch factors below two to avoid fictitious values resulting from the substructure formation.

SPEC. #24 100X

FIGURE 4 APPEARANCE OF FATIGUE CRACK IN TZC SPECIMEN, ANNEALED 3092°F (1700°C), 1 HOUR. TESTED AT AN AMBIENT TEMPERATURE OF 2000°F (1093°F) FOR 4.7×10^9 CYCLES, MURAKAMI'S ETCH

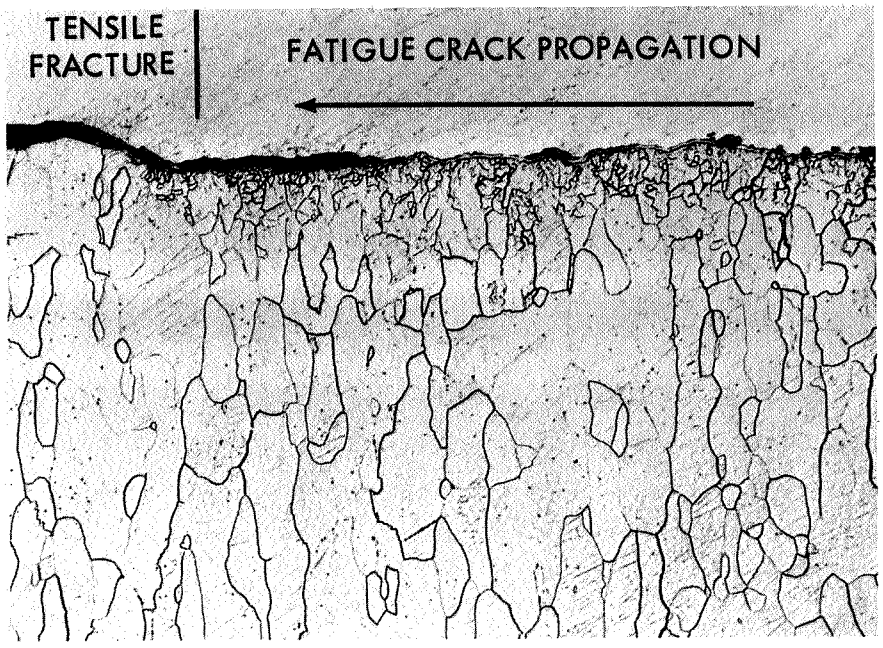

A. TZM SPECIMEN #55, $K_T (D/d)^2 = 2.25$

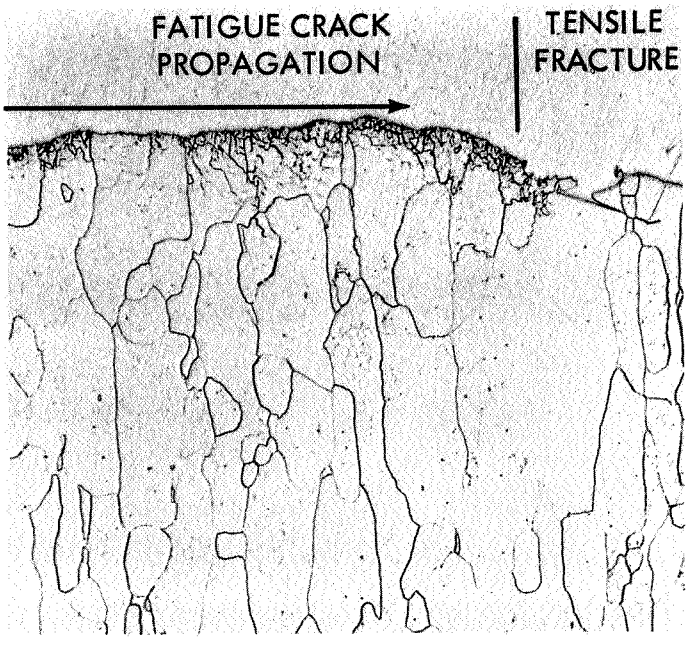

B. TZM SPECIMEN #61, $K_T (D/d)^2 = 1.44$

FIGURE 5 MICROSTRUCTURE AT THE END OF FATIGUE CRACKS IN TZM SPECIMENS - ANNEALED 2850°F (1566°C) FOR 1 HOUR, TESTED AT A = ∞, 2000°F (1093°C) AMBIENT IN VACUUM <1 X 10^{-7} TORR. MURAKAMI'S ETCH 250X

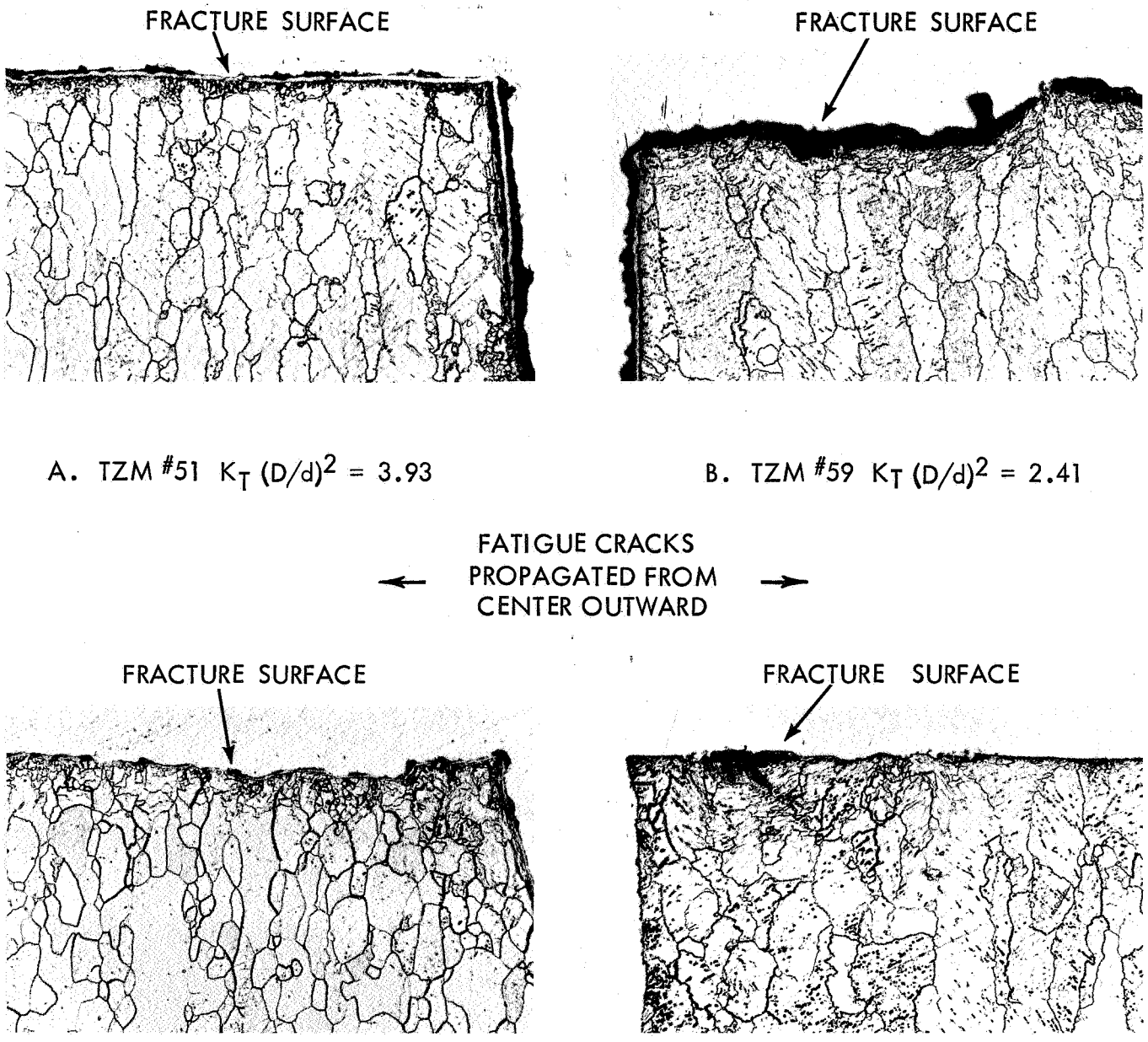

FIGURE 6 MICROSTRUCTURE NEAR FATIGUED CRACK IN TZM SPECIMENS. ANNEALED 2850°F (1566°C) FOR 1 HOUR, TESTED AT A = ∞, 2000°F (1093°C) AMBIENT IN VACUUM $< 1 \times 10^{-7}$ TORR.

MURAKAMI'S ETCH 250 X

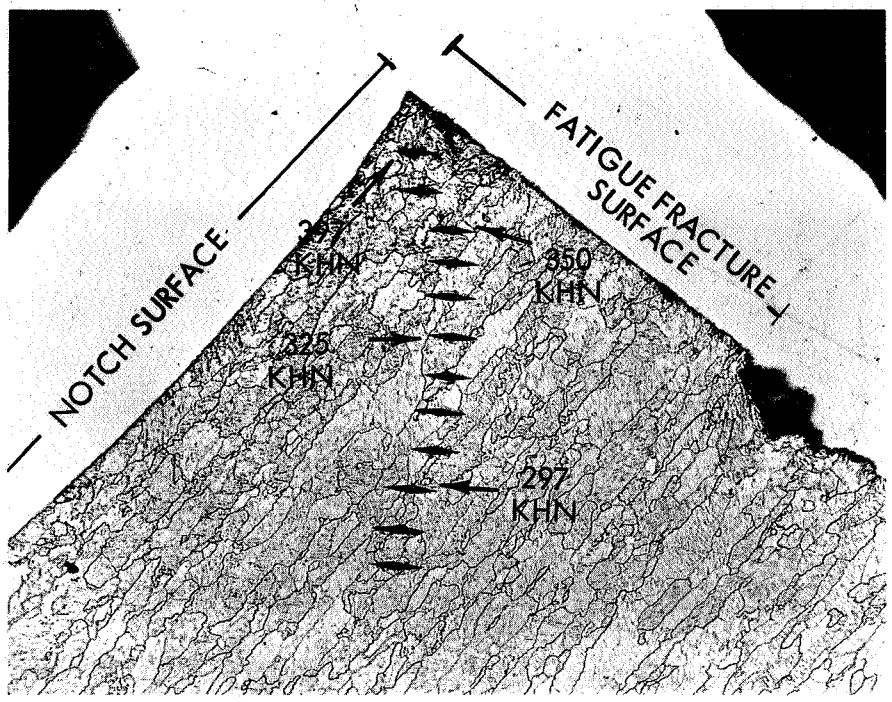

FIGURE 7 TYPICAL LOCATION OF MICROHARDNESS MEASUREMENTS - TZM SPECIMEN NO. 61
$K_T (D/d)^2 = 1.44$

100X MURAKAMI'S ETCH

B. Fatigue and Creep under Dynamic Loading in TZC Alloy

Smooth fatigue specimens of TZC alloy were tested under static loads of 20 Ksi ($1.38 \times 10^8 N/m^2$) at A ratios up to 0.40 at an ambient temperature of 2000°F (1093°C). A detailed drawing of the specimen geometry is shown in Figure 8 and the test data are summarized in Table 3.

Fatigue failures were achieved in specimens of TZC No. 14 and No. 30. The failure in specimen No. 30 is shown in Figures 9A and B. The creep which occurred under the combined static-dynamic load conditions imposed on the smooth specimens of TZC are also listed in Table 3.

The fatigue data for the smooth TZC specimens are plotted in Figure 10 on a Goodman-type diagram developed from previous test results for notched TZC specimens with notch factors of 3.93. The smooth test results at an A ratio of 0.20 agree with the predictions obtained from notch fatigue tests while the result on bar material tested at an A ratio of 0.40 indicates that the notch test predictions of fatigue life are conservative. It has been previously mentioned, that at A ratios of ∞ the notch data tend to underestimate the smooth fatigue life. This behavior probably results from the fact that at the low A ratio (high static loads) a relatively low dynamic stress is required for failure in the notch specimens. Under these conditions the localized effects of strain and temperature produced by the dynamic loading of the sharply notched specimens may not be influential in affecting the fatigue behavior at the lower A ratios.

Since gauge marks cannot be placed on the test specimens without influencing the fatigue life, the creep was measured over the 1.155 inch distance between the specimen shoulders. The creep, however, occurs predominantly over the 0.860 inch specimen gauge section. To compensate for this difference between the measurement distance and the reduced specimen section, a distance of 1.0 inches was arbitrarily selected as the gauge length to calculate the percent creep values. In every case where dynamic load conditions were superimposed on the static load a significant increase in the total creep value was observed. Creep data obtained under both combined dynamic-static loading and solely static loading of TZC (Specimen No. 30, Bar 4230-2) when tested with a 23.8 Ksi peak stress and a A ratio of 0.22 are presented in Figure 11 and Table 4. Also included in the figure are static creep data for specimens from TZC plate of heats M-80 and M-91. These data show a very rapid creep during the first few hours with combined dynamic and static loading, and an appreciable decrease in creep rate when the dynamic load was removed. Similar results have been reported for copper

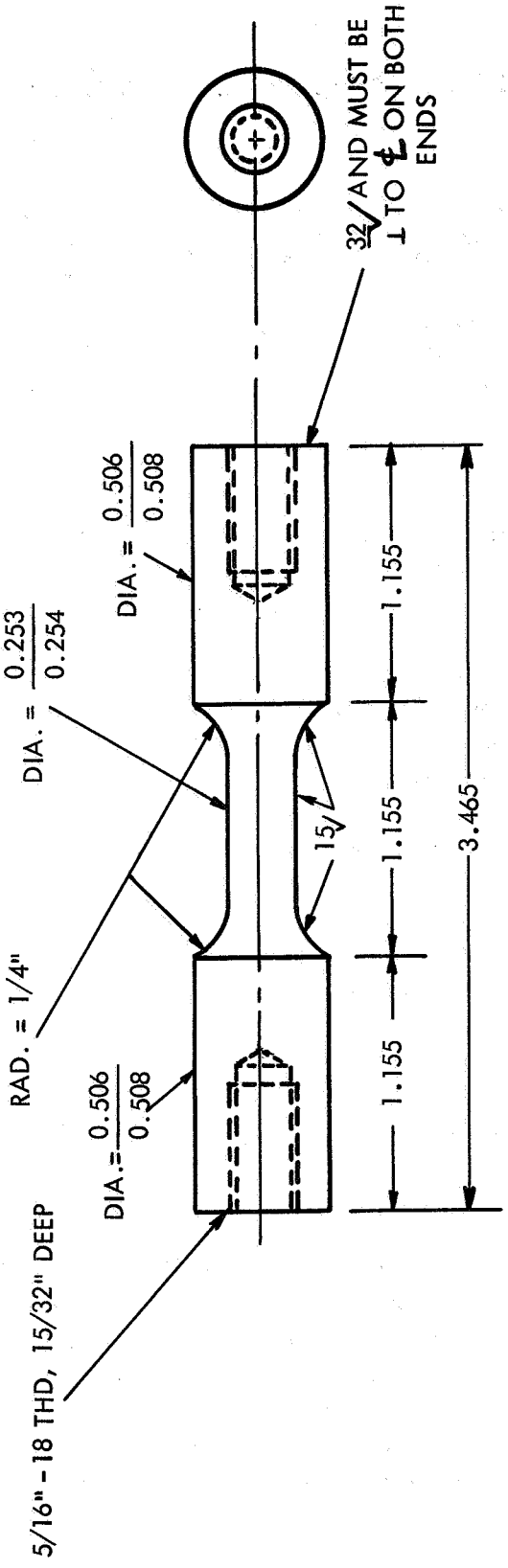

ALL DIAMETER & THD. ENDS MUST BE CONCENTRIC ± 0.002 T.I.R.
USE MINIMUM RELIEF ON THD. ENDS.

FIGURE 8 DUMB-BELL TYPE SMOOTH SPECIMEN GEOMETRY

TABLE 3

Summary of Smooth Fatigue Tests on TZC Bar and Plate, Recrystallized at 3092°F (1700°C), 20 Ksi Static Load, Ambient Test Temperature 2000°F (1093°C), Vacuum Environment $< 1 \times 10^{-7}$ Torr

Specimen	Source	Peak Total Stress (Ksi, $6.89 \times 10^6 N/m^2$)	A-ratio	Fatigue failure Time-Hours	Test* Time (Hrs.)	Dyn. Creep (% in 1")	Temperature Increase, °F
14	M-89	23.9	0.20	37.2	37.2	not measured	0
32	M-91**	<22.0	<0.10	No failure	0.1	2.0	Not measured
34	M-91	22.5	0.12	No failure	26.0	1.4	0
35	M-91	27.2	0.36	No failure	59.3	2.8	20
30	4230-2	23.8	0.22	No failure	599.0	0.4	30
30	4230-2	28.0	0.40	185.0***	185.0	2.3	20
37	4230-2	<22.0	<0.10	No failure	0.05	0.5	Not measured

* Does not include periods of static creep.
** Plate E.
***Fatigue crack showed up during subsequent static loading at 28 Ksi.

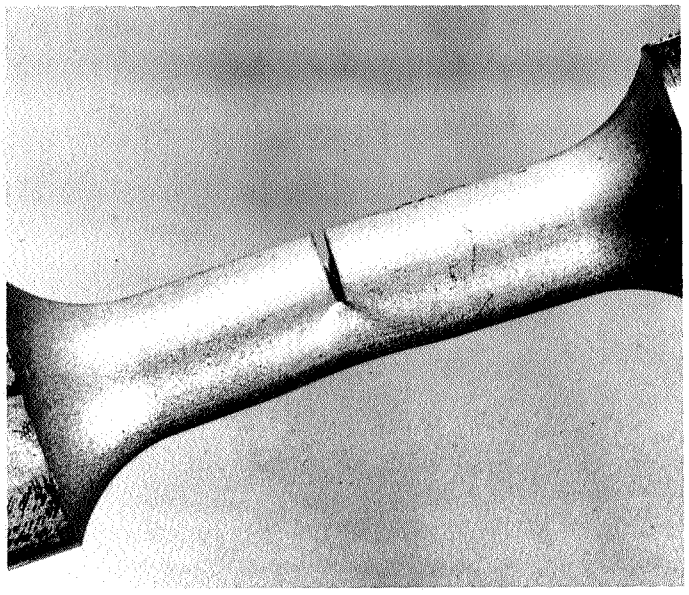

A. SIDE VIEW AT 3X

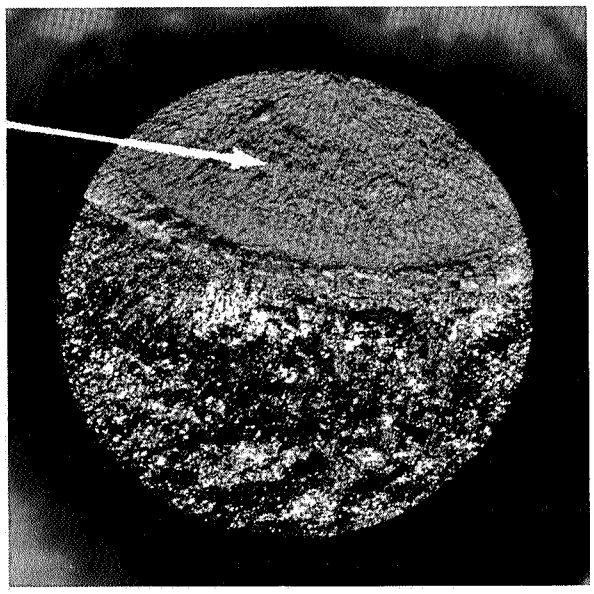

B. FRACTURE SURFACE AT 10X

FIGURE 9 FATIGUE CRACK IN SMOOTH TZC SPECIMEN (BAR 4230-2).

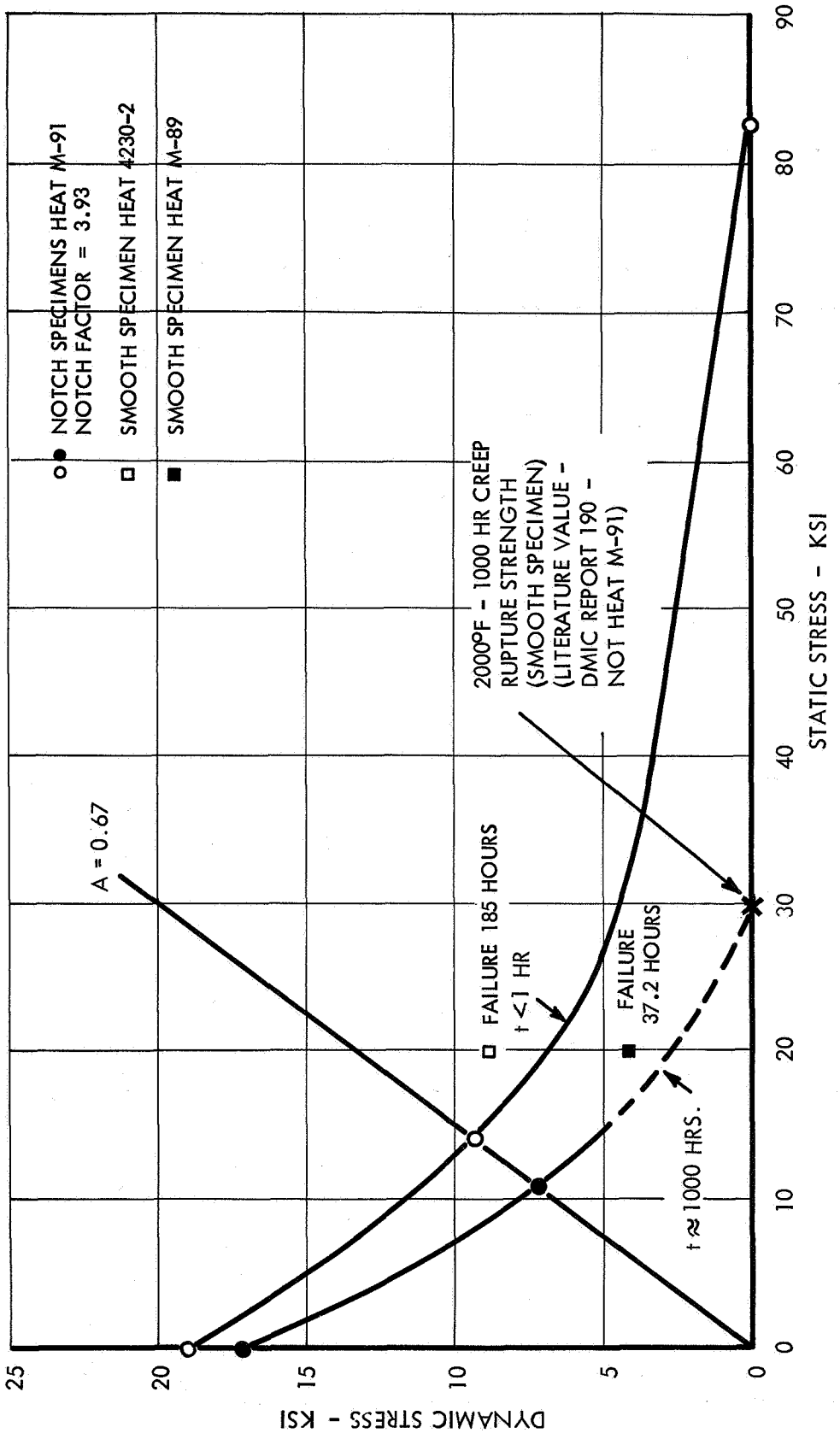

FIGURE 10 GOODMAN DIAGRAM FOR 20KC (20kHz) FATIGUE STRENGTH OF NOTCHED TZC (HEAT M-91) ANNEALED 1 HOUR 1700°C (3092°F), TESTED AT 2000°F (1093°C)

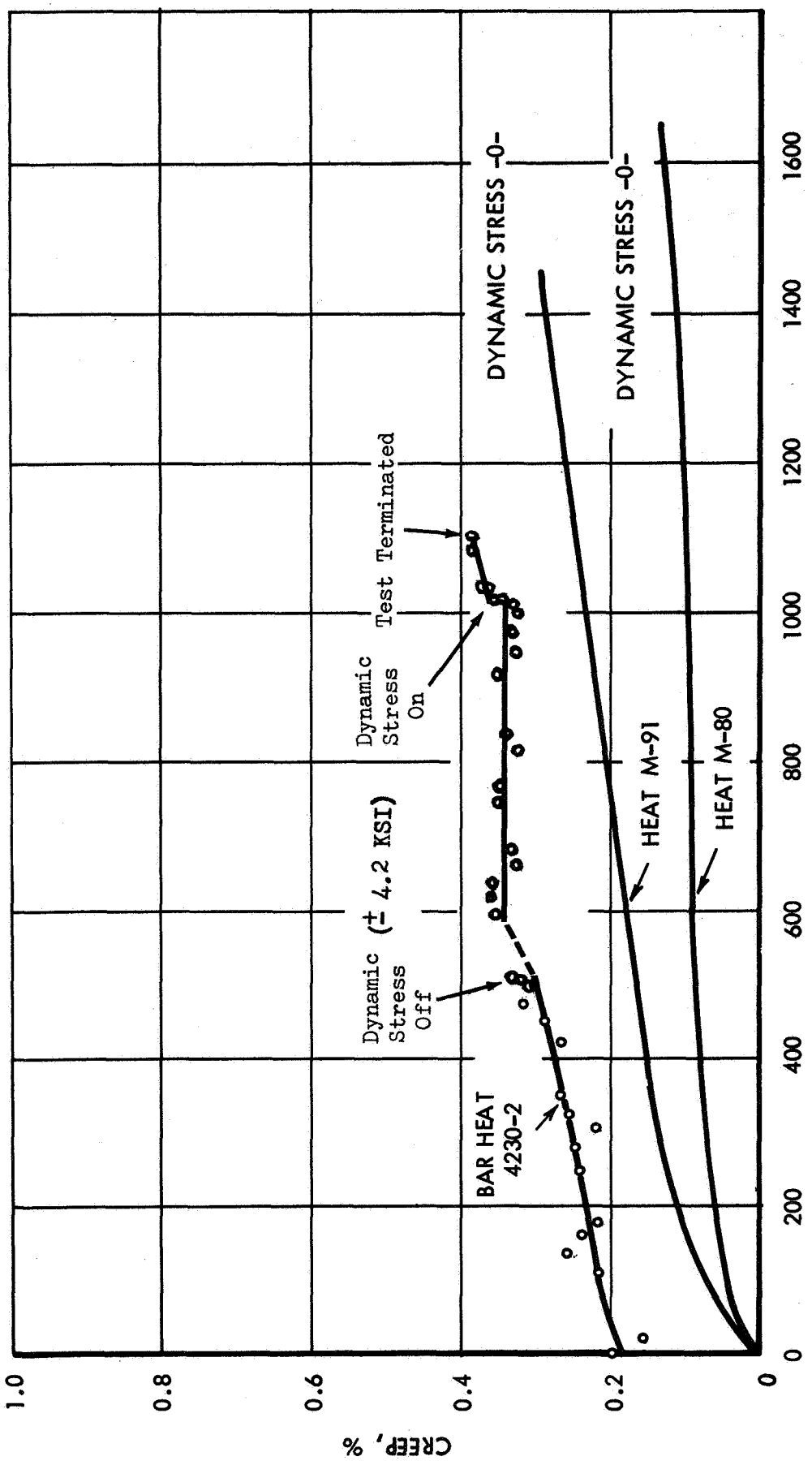

FIGURE 11 CREEP DATA, TZC, ANNEALED 3092°F (1700°C), 1 HOUR. TESTED AT 2000°F (1093°C) AND 20 ksi (1.38×10^8 N/m^2) STATIC STRESS IN VACUUM ENVIRONMENT $< 1 \times 10^{-7}$ TORR.

1728A

TABLE 4

Creep Data TZC Bar (Heat 4230-2) Annealed 3092°F (1700°C), For One Hour, Tested At 2000°F (1093°C), 20 Ksi ($1.38 \times 10^8 N/m^2$) Static Stress, 4.2 Ksi ($2.9 \times 10^7 N/m^2$) Dynamic Stress, and 20 kHz, in Vacuum Environment $< 1 \times 10^{-7}$ Torr

Time (Hrs.)	Length Change inches (1" G. L.)	Creep (%)	Pressure (Torr)
0	0.0000	0	2×10^{-7}
0.1	0.0012	0.12	1×10^{-7}
1.4	0.0020	0.20	5×10^{-8}
18.0	0.0016	0.16	1.7×10^{-9}
110.1	0.0022	0.22	9.6×10^{-9}
134.2	0.0026	0.26	9.5×10^{-9}
158.4	0.0024	0.24	8.1×10^{-9}
182.0	0.0022	0.22	8.5×10^{-9}
253.5	0.0024	0.24	7.8×10^{-9}
278.1	0.0025	0.25	6.6×10^{-9}
304.7	0.0022	0.22	7.2×10^{-9}
326.5	0.0026	0.26	7.3×10^{-9}
350.2	0.0027	0.27	6.7×10^{-9}
422.3	0.0027	0.27	7.0×10^{-9}
446.6	0.0029	0.29	6.7×10^{-9}
470.0	0.0032	0.32	6.3×10^{-9}
494.0	0.0031	0.31	6.2×10^{-9}
500.0	0.0032	0.32	-
500.0	Dynamic Stress Reduced to Zero		
501.0	0.0033	0.33	6.8×10^{-9}
590.0	0.0035	0.35	5.8×10^{-9}
614.1	0.0036	0.36	6.4×10^{-9}
639.2	0.0036	0.36	6.5×10^{-9}
666.8	0.0032	0.32	7.3×10^{-9}
688.0	0.0033	0.33	7.0×10^{-9}
758.2	0.0035	0.35	7.0×10^{-9}
782.5	0.0035	0.35	7.1×10^{-9}
806.0	0.0032	0.32	6.4×10^{-9}
834.7	0.0034	0.34	6.6×10^{-9}
925.0	0.0036	0.36	6.2×10^{-9}
951.0	0.0032	0.32	7.1×10^{-9}
978.0	0.0033	0.33	6.8×10^{-9}
997.1	0.0032	0.32	6.6×10^{-9}
1003.0	0.0033	0.33	-
1003.0	Dynamic Drive Resumed		1.0×10^{-8}
1003.4	0.0035	0.35	-
1004.1	0.0035	0.35	7.5×10^{-9}

TABLE 4 (Continued)

Time (Hrs.)	Length Change inches (1" G. L.)	Creep (%)	Pressure (Torr)
1020.6	0.0034	0.34	7.4×10^{-9}
1025.2	0.0036	0.36	7.5×10^{-9}
1025.8	0.0036	0.36	7.5×10^{-9}
1026.6	0.0037	0.37	7.5×10^{-9}
1027.7	0.0036	0.36	7.4×10^{-9}
1088.1	0.0038	0.38	7.4×10^{-9}
1098.6	0.0038	0.38	7.4×10^{-9}
1103.4	Test Terminated		

by Meleka and Evershed*. The absence of a decrease in length when the dynamic drive was turned off at 500 hours indicates that the high initial creep was not the result of expansion due to self-heating during resonant conditions. In general all of the dynamic creep measurements to date indicate that over 50% of the dynamic creep occurs in the first two hours of test. After extensive amounts of creep, the tests in many cases are terminated prior to fatigue failure since the increase in specimen length results in a loss of resonance and a resultant decrease in the level of dynamic stress. Although the quantity of data is insufficient to allow a quantitative conclusion, the total amount of creep which occurred during the first two hours of test generally increased as the dynamic stress increased. An exception to this behavior was observed in specimen No. 32 where a very large degree of creep extension (2.0%) occurred at a very low dynamic stress level.

To evaluate the relative increase in creep which occurs as a result of the combined dynamic-static load conditions, the data presented in Table 3 were compared on a Larson-Miller plot with static creep data obtained on a related NASA program (NAS 3-2545). In this comparison, which is shown in Figure 12, the dynamic-static creep data are plotted at a temperature which is the ambient temperature plus the temperature increase due to the high frequency loading. In cases where no temperature increase was measured the ambient test temperature was employed. The dynamic-static data are plotted as a stress range to indicate both the peak and average stress conditions. With the exception of specimen No. 30, the presence of a dynamic load superimposed on a static load resulted in a significant increase in the total creep value, and the degree of creep obtained under the combined loading conditions is greater than that obtained only under static conditions at the peak stress value.

---

* A. H. Meleka and A. V. Evershed, "The Dependence of Creep Behavior on the Duration of a Superimposed Fatigue Stress," J. of Institute of Metals, Vol. 88, pp. 411-414.

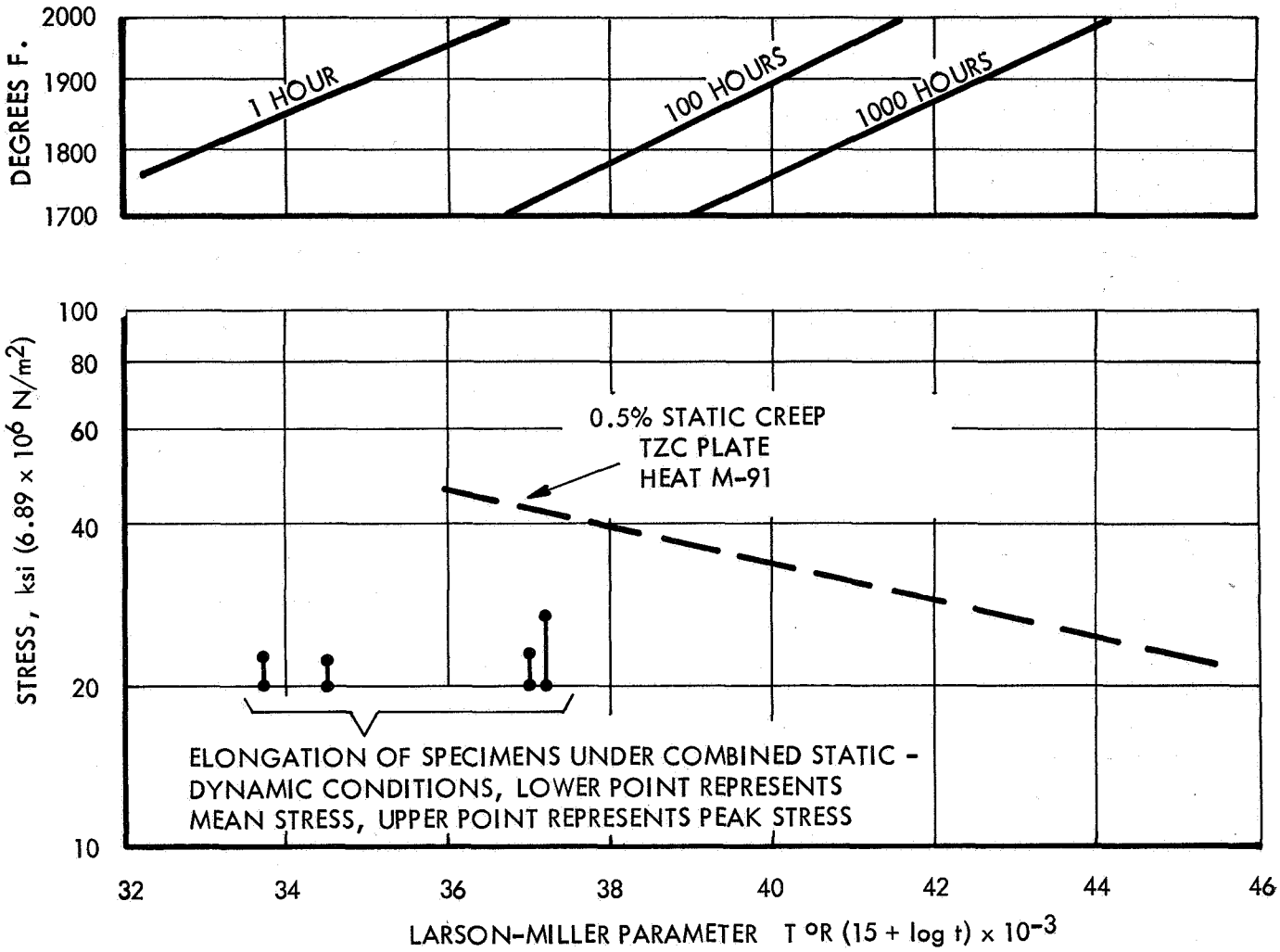

FIGURE 12 COMPARISON OF CREEP OBTAINED UNDER STATIC CONDITIONS WITH THAT OBTAINED UNDER COMBINED DYNAMIC-STATIC LOADING. TZC ALLOY, TESTED IN VACUUM ENVIRONMENT $<1 \times 10^{-7}$ TORR.

IV FUTURE WORK

The tests of TZM alloy specimens with varying notch geometries will be completed. In addition, fatigue tests will continue on smooth specimens of TZC alloys for the simultaneous determination of fatigue strength and dynamic creep rate at relatively low A ratios. Additional metallographic studies will be made of the substructure along the fatigue crack in notched specimens of TZM and TZC. Additional TZC test material has been ordered and will be included in the evaluation program.